PHYSICAL REVIEW C **72**, 022202(R) (2005)

The Primakoff effect on a proton target

J. M. Laget*

Thomas Jefferson National Accelerator Facility, Newport News, Virginia 23606, USA

(Received 1 March 2005; published 17 August 2005)

The Primakoff effect offers us a way to determine the radiative decay width of pseudoscalar mesons when they are photoproduced in the electromagnetic field of hadronic systems. Taking advantage of recent developments in the Regge description of the production of mesons in the strong hadronic field, this paper evaluates the relative importance of the electromagnetic and the strong amplitudes and assesses the possibilities that have become opened because of modern experimental facilities.

DOI: 10.1103/PhysRevC.72.022202 PACS number(s): 13.60.Le, 12.40.Nn

The study of the Primakoff effect [1] in the coherent photoproduction of pseudoscalar mesons on nuclear targets has been recently completed at JLab [2] and will greatly benefit from its energy upgrade to 12 GeV [3]. The production of a meson in the Coulomb field of the nuclear target gives direct access to its radiative decay. A precise knowledge of the π°-meson radiative decay provides an accurate test of chiral anomalies and mixing effects that are due to isospin breaking by the difference of the masses of light quarks [4]. The precise measurement of the radiative widths of the η and η' mesons will lead to an absolute determination of their other decay widths, which are usually measured relative to the radiative decay width. A better understanding of the (π°, η, and η') system will result in the determination of the mixing angles that quantify isospin and SU(3) symmetry breaking [4].

However, the mesons can be concurrently photoproduced in the strong nuclear field. This hadronic interaction is mediated by the exchange of vector mesons (ρ and ω) whose singularity is more distant from the physical region than the singularity of the photon that is exchanged in the Primakoff amplitude. Consequently, the strong amplitude contributes to large production angles, but its tail must be subtracted from the Primakoff amplitude, which contributes at smaller angles. In previous pioneering experiments [5,6], this has been achieved by parametrizing the experimental yield at large angles and extrapolating it below the Primakoff peak. While this procedure led to a radiative decay width of the π° meson that was in good agreement with the value deduced from collider experiments, it led to a radiative width of the η meson that was about two times smaller [7].

The quality of the beam of CEBAF at JLab, and the improvement in the experimental setup permit the study of the Primakoff production of pseudoscalar mesons and the determination of their radiative decay widths with an unprecedented statistical, as well as systematic, accuracy. Mastering the hadronic contribution becomes mandatory. This note is an attempt to determine the relative importance and the interplay between the Primakoff effect and the strong amplitude on the simplest target, the proton. It takes advantage of the latest developments [8] in the Regge description of the photoproduction of π° meson and its extension to the η and η' sectors.

Let us start with the π° production channel. Figure 1 summarizes the results at $E_\gamma = 5.8$ GeV, where experimental data [9,10] exist. The cross sections are plotted against the squared four-momentum transfer $t = (k_\gamma - p_{\pi^\circ})^2$ between the incident photon [$k_\gamma = (E_\gamma, \boldsymbol{k}_\gamma)$] and the outgoing meson [$p_{\pi^\circ} = (E_{\pi^\circ}, \boldsymbol{p}_{\pi^\circ})$]. Since the energy is large and the mass of π° is small, the minimum value, $t_{\min}$, of $-t$ is very small, and the Primakoff peak is well separated from the hadronic peak. The experimental data seem to prefer a constructive (solid curve) rather a destructive (dotted) interference between the two contributions, but the tail of the hadronic amplitude does not affect the Primakoff peak at all in the range of small $-t$ where it dominates.

Quantitatively, the hadronic amplitude is the same as in Ref. [8], where its detailed expression and an extended discussion on the choice of the vertices and coupling constants can be found. Suffice it to say that the amplitude is based on the exchange of the Regge trajectories of the ρ and ω mesons and takes into account the full spin–isospin structure of the electromagnetic and the strong vertices. We have chosen a degenerate Regge propagator for the ω in order to accommodate the minimum in the experimental angular distribution around $-t = 0.5$ GeV^2:

$$\mathcal{P}_\omega = \left(g^{\mu\nu} - \frac{k_\omega^\mu k_\omega^\nu}{m_\omega^2}\right)\left(\frac{s}{s_\circ}\right)^{\alpha_\omega(t)-1} \frac{\pi\alpha'_\omega}{\sin[\pi\alpha_\omega(t)]}\frac{1}{\Gamma[\alpha_\omega(t)]} \times \frac{1+\exp[-i\pi\alpha_\omega(t)]}{2}, \quad (1)$$

where the ω Regge trajectory is

$$\alpha_\omega(t) = 0.44 + 0.9t \quad (2)$$

and $s_\circ = 1$ GeV is a mass scale. The Gamma function $\Gamma[\alpha(t)]$ suppresses the singularities in the physical region ($t < 0$). The strong coupling constants are $g^2_{\omega NN}/4\pi = 17.9$ and $\kappa_\omega = 0$.

For the ρ, we chose a degenerate propagator with a rotating phase:

$$\mathcal{P}_\rho = \left(g^{\mu\nu} - \frac{k_\rho^\mu k_\rho^\nu}{m_\rho^2}\right)\left(\frac{s}{s_\circ}\right)^{\alpha_\omega(t)-1} \frac{\pi\alpha'_\rho}{\sin[\pi\alpha_\rho(t)]}\frac{1}{\Gamma[\alpha_\rho(t)]} \times \exp[-i\pi\alpha_\rho(t)], \quad (3)$$

*Corresponding author: laget@jlab.org (J. M. Laget)

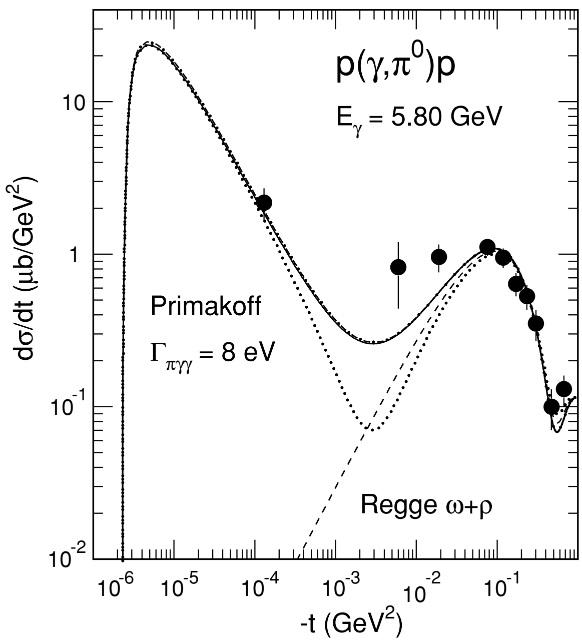

FIG. 1. Angular distribution of the π° mesons photoproduced in the reaction $p(\gamma,\pi^\circ)p$, at $E_\gamma = 5.8$ GeV. The dashed curve corresponds to the hadronic cross section, while the solid curve corresponds to the coherent sum of the electromagnetic and the hadronic amplitudes. The sign of the electromagnetic amplitude has been changed in the dotted curve.

where the ρ Regge trajectory is

$$\alpha_\rho(t) = 0.55 + 0.8t. \tag{4}$$

The strong coupling constants are $g^2_{\rho NN}/4\pi = 0.92$ and $\kappa_\rho = 6.1$.

The coupling constant of the electromagnetic vertex (as defined in Ref. [8]) is related to the corresponding decay width of the vector meson through the expression

$$\Gamma_{V\to\pi\gamma} = \frac{\alpha_{\rm em}\left(m_V^2 - m_\pi^2\right)^3}{24 m_V^3 m_\pi^2}\, g^2_{V\pi\gamma}. \tag{5}$$

This gives $g_{\omega\pi\gamma} = 0.314$, for $\Gamma_{\omega\to\pi\gamma} = 720$ keV, and $g_{\rho\pi\gamma} = 0.103$, for $\Gamma_{\rho\to\pi\gamma} = 68$ keV [8].

It turns out that the contraction between the mass-dependent term $k^\mu_\rho k^\nu_\rho/m^2_\rho$ of the vector meson propagator and the electromagnetic vertex vanishes, and only the contribution of the $g^{\mu\nu}$ part survives. Therefore the Primakoff amplitude takes the same form as the vector meson exchange amplitudes, provided that the Regge propagator is replaced by the Feynman propagator of the photon,

$$\mathcal{P}_\gamma = g^{\mu\nu}/t, \tag{6}$$

and the strong coupling constants by $g^2_{\gamma NN}/4\pi = \alpha_{\rm em}$ and $\kappa_\gamma = 1.79$. The Primakoff coupling constant is related to the two-photon decay width as follows:

$$\Gamma_{\pi\to\gamma\gamma} = \frac{\alpha_{\rm em} m_\pi}{16}\, g^2_{\pi\gamma\gamma}. \tag{7}$$

The solid curve in Fig. 1 corresponds to the central value $\Gamma_{\pi\to\gamma\gamma} = 8$ eV of Ref. [7] ($g_{\pi\gamma\gamma} = 0.0114$), while the dotted and dashed curves uses 8.4 eV at the edge of the experimental values.

Because of the structure of the electromagnetic vertices, both the hadronic amplitude and the Primakoff amplitudes strickly vanish at $\theta_\pi = 0$ and therefore at $t_{\rm min}$. However, the photon pole is so close to the physical region that it boosts the Primakoff amplitude orders of magnitude above the strong amplitude.

The b_1-meson exchange may also contribute to the strong amplitude. In Ref. [8] we found that, while it is necessary to reproduce the beam asymmetry, it only modifies the unpolarized cross section by about 10% in the region of the minimum ($-t \sim 0.5$ GeV^2) and above. So it may modify the strong amplitude by the same amount below $-t \sim 10^{-3}$ GeV^2. Since our knowledge of its coupling constants is on less solid ground than those of ρ and ω mesons, I do not retain its contribution.

The model confirms the earlier estimate of the cross section that was included in the experimental papers [9,10]. While there is no reason that the Primakoff amplitudes should be different, the strong amplitude included exchanges of the ω- and b_1-meson Regge trajectories and the ω Pomeron cut, following Refs. [11,12]. The residues of the poles were fitted to the data, contrary to the model which I use: in Ref. [8] we chose the values of strong and electromagnetic coupling constants in the range of values determined in independent channels, and we implemented the full spin–isospin structure of the lower mass realization of each Regge trajectory.

In Fig. 1 the experimental points have been plotted at the mean value of $-t$ in each experimental bin in θ_{π°. This is model dependent. Although the model used in Ref. [9] is very similar, a new experimental determination of the π° Primakoff cross section, with a better angular resolution, is highly desirable, especially in the domain where the Primakoff and the strong amplitudes interfere.

Increasing the energy up to $E_\gamma = 9$ GeV does not change the picture dramatically. As can be seen in Fig. 2, $t_{\rm min}$ decreases by a factor of two, but this does not improve the separation between the Primakoff and the hadronic peak, which was already very good at 5.8 GeV. Note that the Regge model reproduces the experimental data quite well [13] at this energy also.

In contrast, increasing the energy helps in the η and η' channels. Figure 3 shows the angular distribution of the η mesons emitted in the $p(\gamma,\eta)p$ reaction at $E_\gamma = 6$ GeV. The value of $t_{\rm min}$ is more than 2 orders of magnitude bigger than in the π° channel. Consequently, one has to rely on the tail of the Primakoff amplitude, which shows up above the tail of the strong amplitude.

The model uses the same ρ exchange amplitude [degenerate Regge propagator, Eq. (3), with the same strong coupling constants) as in the π° channel. The radiative coupling constant $g_{\rho\eta\gamma} = 0.81$ is deduced from the experimental decay width $\Gamma_{\rho\to\eta\gamma} = 39$ keV [7] with Eq. (5) (where the π mass is replaced by the η mass, m_η).

In the ω exchange amplitude, the radiative decay constant $g_{\omega\eta\gamma} = 0.29$ is also fixed by the experimental decay width $\Gamma_{\omega\to\eta\gamma} = 5.4$ keV [7]. But, following Ref. [14], I use the degenerate form, Eq. (3), instead of the nondegenerate form,

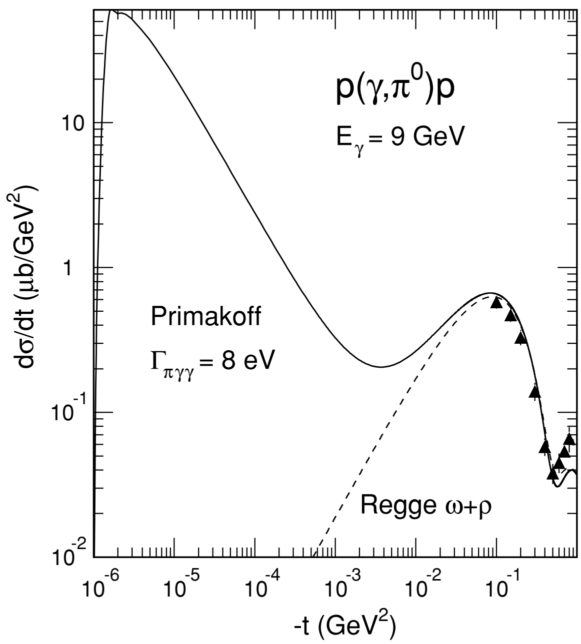

FIG. 2. Angular distribution of the π° mesons photoproduced in the reaction $p(\gamma,\pi^\circ)p$, at $E_\gamma = 9$ GeV. The meaning of the curves is the same as in Fig. 1.

which I used in the π° channel. The reason is that available experimental data [15] do not exhibit a minimum in the vicinity of the first node of the ω nondegenerate Regge trajectory. In nature, Regge trajectories [in the form of Eq. (1)] go by pair, each having the same slope but a different signature, $S = \pm 1$, when it connects members with either odd or even spins. When it happens that each trajectory has the same, or comparable, coupling constants as the probe, they combine into a degenerate trajectory with or without a rotating phase [Eq. (3)]. Only experiment tells us what is the best choice. The conjecture is that the photon couples to a degenerate trajectory of the ω in the η photoproduction channel, while it couples to a nondegenerate ω trajectory in the π° sector. Consequently the strong coupling constants of the ω are not necessarily the same in both channels. A good agreement with the data is achieved when I use $g^2_{\omega NN}/4\pi = 6.44$ and I keep $\kappa_\omega = 0$.

This set of coupling constants is different from the set of Ref. [14], which were obtained from a global fit in the η and η' sector. I prefer to use a set that differs in a minimal way from the π° sector set. It is worth noting that both sets lead to a similar accounting of the strong part of the cross section.

The Primakoff coupling constant of the η meson, $g_{\eta\gamma\gamma} = 0.0429$, is deduced from the average (including Primakoff measurement) value $\Gamma_{\eta\to\gamma\gamma} = 0.46$ keV of Ref. [7] with the help of Eq. (7) (where the π-meson mass is replaced by the η-meson mass).

The experimental study of the Primakoff effect will greatly benefit from an increase of the incoming photon energy. Figure 4 clearly demonstrates that, at $E_\gamma = 11$ GeV, $t_{\rm min}$ is lowered by about a factor of three and that the Primakoff peak is clearly separated from the strong hadronic peak. In the meantime, the measurement should be repeated at $E_\gamma = 6$ GeV. The accepted t interval, FWHM as given in Ref. [15], has been plotted in Fig. 3. Clearly a much better angular resolution is necessary for a sensible check of the strong amplitude at the most forward angles.

Let us turn now to the η' channel, where I keep the same amplitudes as in the η channel and only change the radiative coupling constants. The η' radiative decay to the ρ or the ω mesons is related to the radiative coupling constant in

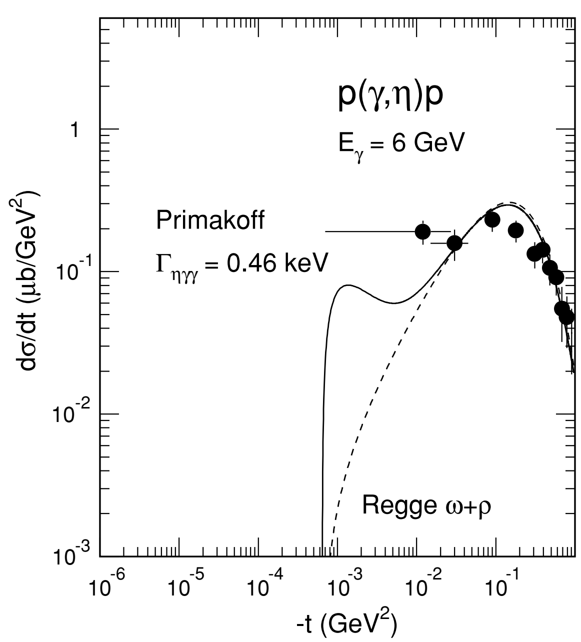

FIG. 3. Angular distribution of the η mesons photoproduced in the reaction $p(\gamma,\eta)p$, at $E_\gamma = 6$ GeV. The meaning of the curves is the same as in Fig. 1.

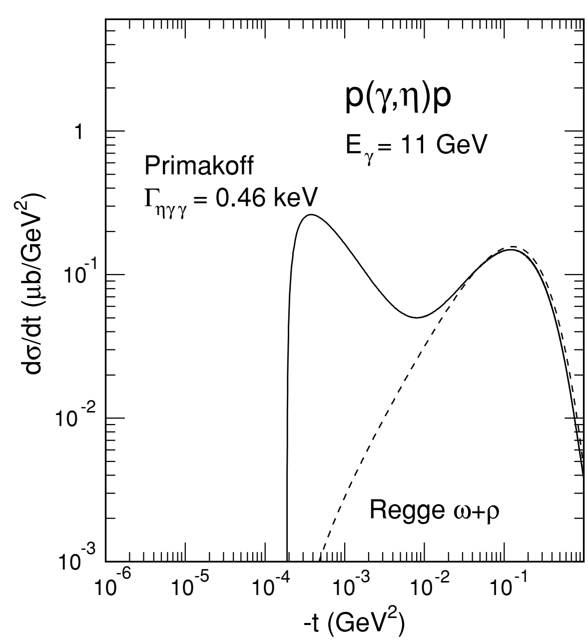

FIG. 4. Angular distribution of the η mesons photoproduced in the reaction $p(\gamma,\eta)p$, at $E_\gamma = 11$ GeV. The meaning of the curves is the same as in Fig. 1.

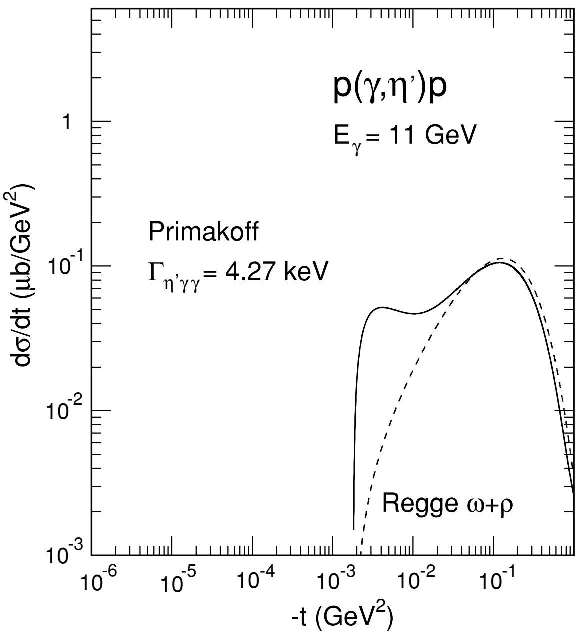

FIG. 5. Angular distribution of the η' mesons photoproduced in the reaction $p(\gamma,\eta')p$, at $E_\gamma = 11$ GeV. The meaning of the curves is the same as in Fig. 1.

the following way:

$$\Gamma_{\eta'\to V\gamma} = \frac{\alpha_{\rm em}\left(m_{\eta'}^2 - m_V^2\right)^3}{8m_{\eta'}^5}\, g_{V\eta'\gamma}^2. \quad (8)$$

This corresponds to $g_{\omega\eta'\gamma} = 0.43$, for $\Gamma_{\eta'\to\omega\gamma} = 6$ keV, and $g_{\rho\eta'\gamma} = 1.24$, for $\Gamma_{\eta'\to\rho\gamma} = 55$ keV.

Again the Primakoff coupling constant of the η' meson, $g_{\eta'\gamma\gamma} = 0.0989$, is deduced from the central value $\Gamma_{\eta'\to\gamma\gamma} = 4.27$ keV of Ref. [7] with the help of Eq. (7) (where the π-meson mass is replaced by the η'-meson mass).

The results are shown in Fig. 5 at $E_\gamma = 11$ GeV. Even at such a high energy, $t_{\rm min}$ is high and the Primakoff contribution appears as a shoulder on the tail of the strong amplitude. The situation is similar to that in the η sector at $E_\gamma = 6$ GeV. Certainly an experiment with an excellent energy resolution will disentangle the Primakoff amplitude at the lowest angles, where it overwhelms by more that an order of magnitude the strong amplitude, which will be calibrated at higher angles.

Unlike data for the π° and the η channels, the experimental data set is extremely scarce. The model can be compared only to integrated experimental cross sections [16,17]. At $E_\gamma =$ 5 GeV, it predicts $\sigma = 0.1$ μb in the range of the experimental cross section $\sigma_{\rm exp} = 0.17 \pm 0.12$ μb. This gives confidence in its extrapolation from the η to the η' channel. But a more accurate determination of the angular distribution is definitely needed.

In conclusion, the Regge description of the strong hadronic amplitude has been extended from π° to η and η' photoproduction. It reproduces all the available experimental data and provides us with a solid starting point for evaluating the hadronic contribution below the Primakoff peak. The Primakoff amplitude has been incorporated into the model. While in the π° sector it is prominent already at $E_\gamma = 6$ GeV, its determination in the η and η' sector requires accurate experiments at higher energies.

I thank A. Bernstein and R. Miskimen, who triggered my interest in the Primakoff effect, J. Goity who taught me its relevance to QCD, and M. Vanderhaeghen for discussions on Regge models.

[1] H. Primakoff, Phys. Rev. **81**, 899 (1951).
[2] D. Dale *et al.*, PRIMEX Experiment, JLab-E-02-103.
[3] Pre-Conceptual Design Report (pCDR) for the Science and Experimental Equipment for the 12 GeV Upgrade of CEBAF (JLab, April 2003).
[4] J. L. Goity, A. M. Bernstein, and B. R. Holstein, Phys. Rev. D **66**, 076014 (2002).
[5] A. Browman *et al.*, Phys. Rev. Lett. **33**, 1400 (1974).
[6] A. Browman *et al.*, Phys. Rev. Lett. **32**, 1067 (1974).
[7] S. Eidelman *et al.*, Phys. Lett. **B572**, 1 (2004).
[8] M. Guidal, J. M. Laget, and M. Vanderhaeghen, Nucl. Phys. **A627**, 645 (1997).
[9] M. Braunschweig *et al.*, Phys. Lett. **B26**, 405 (1968).
[10] M. Braunschweig *et al.*, Nucl. Phys. **B20**, 191 (1970).
[11] J. P. Ader, M. Capdeville, and Ph. Salin, Nucl. Phys. **B3**, 407 (1967).
[12] A. Capella and J. Tran Thanh Van, Nuovo Cimento Lett. **1**, 321 (1969).
[13] R. Anderson *et al.*, Phys. Rev. D **1**, 27 (1970).
[14] W.-T. Chiang, S. N. Yang, L. Tiator, M. Vanderhaeghen, and D. Drechsel, Phys. Rev. C **68**, 045202 (2003).
[15] W. Braunschweig *et al.*, Phys. Lett. **B33**, 236 (1970).
[16] ABBHHM Collaboration, Phys. Rev. **175**, 1669 (1968).
[17] W. Struczinski *et al.*, Nucl. Phys. **B108**, 45 (1976).